

CHEMICAL RESEARCH IN TOXICOLOGY (ISSN: 0893-228X) 27: (5) pp. 765-774. (2014)

DOI: 10.1021/tx4004227

Radical Model for Arsenic Toxicity: Experimental EPR Spin Trapping and Theoretical Studies

Pedro L. Zamora^a, Antal Rockenbauer^b, and Frederick A. Villamena^{a}*

[†] Department of Pharmacology, The Davis Heart and Lung Research Institute, College of Medicine, The Ohio State University, Columbus, Ohio 43210, United States

[‡] Department of Physics, Budapest University of Technology and Economics and MTA-BME Condensed Matter Research Group, Budafoki ut 8, 1111 Budapest, Hungary

Keywords: arsenic, arsenite, monomethylarsonous acid, dimethylarsinous acid, MMA, DMA,

Abstract

* Correspondence to: Frederick.Villamena@osumc.edu , Fax: (614)-292-688-0999

Arsenic is one of the most environmentally significant toxins and a great global health concern. Long known for its acute toxicity, arsenic has also been discovered to be a potent carcinogen. Evidence links arsenic toxicity and carcinogenic actions to reactive oxygen species (ROS). In most animal including humans, arsenic undergoes a biomethylation to yield organic arsenic species, long assumed to be a process of detoxification. However, a growing body of evidence suggests that these organic arsenic species, particularly the reduced trivalent intermediates, may be just as if not more toxic than the inorganic analogs. Furthermore, current food safety regulations often monitor only inorganic arsenic levels. There is, therefore, a clear need for more literature and empirical data concerning the toxic mechanisms of arsenic.

In this study, we examined organic and inorganic arsenites capacity to generate ROS when exposed to common oxidizing agents *via* EPR spectroscopy and spin-trapping with the cyclic nitron 5,5-dimethyl-1-pyrroline-*N*-oxide (DMPO). Experimental observations were theoretically rationalized using density functional theory approach.

Introduction

As a naturally occurring element abundant in the earth's crust, arsenic and its compounds are environmentally pervasive health hazards. Long known for its acute toxicity, arsenic is also understood to act as a potent carcinogen, even at sublevel concentrations. Studies of long-term exposure in humans associate arsenic with skin, bladder, lung, liver, colon, prostate, and kidney cancers.¹⁻⁵ Besides a possible role in causing cancer, arsenic exposure has also been linked to hypertension, cardiovascular diseases, diabetes, and the unique vaso-occlusive Blackfoot disease^{6,7} where undernourished populations are believed to be at a higher risk for developing these conditions.⁸ Hence, the monitoring of levels of arsenic in food, water, and soil is of tremendous importance, particularly in developing countries. The urgency of this global health initiative has renewed interest in arsenic chemistry, particularly for the purposes of elucidating the mechanism of its carcinogenic properties.

Inorganic arsenic in the environment typically exists as the pentavalent As^{V} (arsenic acid, H_3AsO_4) or the trivalent As^{III} (arsenous acid, H_3AsO_3).⁹ Of the two forms, As^{III} (or as it is more commonly named by its conjugate base arsenite) is more toxic and mobile and remains in tissues longer.¹⁰ Once inhaled or ingested, inorganic arsenic is transformed to organic arsenic *via* a series of enzyme-catalyzed successive reduction and methylation steps (Scheme 1).^{11, 12} Initially believed to be a detoxification mechanism, it has been realized that the organic trivalent arsenic species monomethylarsonous acid (MMA^{III}) and dimethylarsinous acid (DMA^{III}) are the most toxic of all arsenic metabolites detected in human and animal urine.¹³⁻¹⁷ Variations at certain points in the human arsenic methyltransferase (*AS3MT*) gene may cause differences in methylating ability between individuals,¹⁸ but data suggests a standard profile of urinary arsenic in humans as 10-30% inorganic, 10-20% $\text{MMA}^{(\text{III}+\text{V})}$, and 60-80% $\text{DMA}^{(\text{III}+\text{V})}$.¹⁹ The acute toxicity

of inorganic As^V has been understood in its capacity to replace phosphate in biomolecules and to uncouple ATP *via* so-called arsenolysis. Compounding the lack of information is the apparent paradoxical dual-action of arsenic as both carcinogen and chemotherapeutic agent. Despite the plethora of evidence linking arsenic exposure to the development of various cancers, inorganic arsenite remains one of the most effective treatments for certain cancers, including acute promyelocytic leukemia (APL).²⁰⁻²⁴

A growing body of evidence suggests that both the apoptosis-inducing antitumor effects and the genotoxic effects of arsenite and other arsenic metabolites are mediated *via* ROS and oxidative stress pathways.^{5, 25-35} Recent evidence also suggests that biomethylation of arsenic may be responsible for the observed carcinogenicity.^{36, 37} However, it is currently not known which specific form (or forms) of arsenite is responsible for the observed antitumor and genotoxic effects due to the various transformations arsenic undergoes *in vivo*. Furthermore, there is a current lack of literature concerning the structural differences between the organic and inorganic arsenites and the effects of structure on capacity to generate ROS. Gaining greater understanding of the electronic properties, reactivities, and differences therein of the inorganic and organic arsenic radical species may help to elucidate arsenic's toxic mechanisms. We used electron paramagnetic resonance (EPR) spectroscopy and the spin trap 5,5-dimethyl-1-pyrroline-*N*-oxide (DMPO) to study the free radical activity of As^{III} and DMA^{III} in aqueous solution. We also performed theoretical calculations on the structures and thermodynamics of the arsenic species involved in several proposed mechanisms of oxidation and radical generation as well as theoretical analysis of the spin adducts experimentally generated. We have identified trends in ROS activity that closely correlate to trends in the experimental data as a function of degree of methylation.

Experimental Procedures

General Computational Methods. All calculations were performed at the Ohio Supercomputer Center using Gaussian 09.³⁸ Density functional theory^{39,40} was applied in this study to determine the optimized geometry, vibrational frequencies, and single-point energy of all stationary points.⁴¹⁻⁴⁴ Single-point energies were obtained at the B3LYP/6-31+G** level based on the optimized B3LYP/6-31G* geometries, and the B3LYP/6-31+G**// B3LYP/6-31G* wave functions were used for Natural Population Analyses (NPA).⁴⁵ The effect of solvation on the gaseous phase calculations was also investigated using the polarizable continuum model (PCM).⁴⁶⁻⁵⁰ The B3LYP level was employed based on previous studies demonstrating the appropriateness of this level for the study of H₂AsO radical compared to other more powerful levels of theory.⁵¹ The 6-31G* basis set was chosen for its computational speed and its good agreement with experimentally determined bond lengths and angles for the third row atoms.⁵² These basis set calculations used the standard six Cartesian d functions. Vibrational frequency analyses (B3LYP/6-31G*) for each of the stationary points for all arsenic species and for DMPO and its spin adducts yielded no imaginary vibrational frequencies. A scaling factor of 0.9806 was used for the zero-point vibrational energy (ZPE) corrections with the B3LYP/6-31G*.⁵³

Calculation of Isotropic Hyperfine Coupling Constants (hfcc). The prediction of hfcc of the nitrogen atom in simple nitroxides was demonstrated in several benchmark works.^{49, 54-56} Based on these previous studies, we employed similar models in the prediction of hfcc's of the nitrogen, β -hydrogen and γ -hydrogens of possible DMPO adducts of radical species produced by the oxidation of As^{III} and DMA^{III} in water. A discussion of the comparative study of the calculated hfcc's for DMPO-O₂H optimized at the B3LYP density functional and basis sets, 6-31+G**, 6-31G*, EPR-II and EPR-III,⁵⁷ and the core-valence correlation-consistent cc-pCVDZ⁵⁸

in the gas and aqueous phases can be found in pages S13-S18 of the Supplementary Material Section of our previous paper.⁵⁹ In the same article,⁵⁹ the hybrid PBE0 functional and EPR-II basis set was found⁵⁶ to yield accurate a_N values in simple nitroxides and was also employed in the calculation of hfcc's for DMPO-O₂H. Although the levels of theory mentioned above gave accurate a_N for 2,2,5,5-substituted pyrrolidine nitroxides, the calculated hfcc's for DMPO-O₂H using the same levels of theory gave hfcc's comparable to that predicted at B3LYP/6-31+G**//B3LYP/6-31G*. Hence, in this study, the a_N , $a_{\beta-H}$ and $a_{\gamma-H}$ for all of the spin adducts were only calculated at the B3LYP/6-31+G**//B3LYP/6-31G* level to show *qualitative* trends in the hfcc compared to the experimental.

EPR Measurements. EPR measurements were carried out on an X-band spectrometer with HS resonator at room temperature. General instrument settings are as follows unless otherwise noted: microwave power, 10 mW; modulation amplitude, 0.5 G; receiver gain 3.17-3.56 x 10⁵, time constant, 82 ms, time sweep 42 s. The hyperfine splittings (hfcc) of the spin adducts were determined by simulating the spectra using an automatic fitting program.⁶⁰

Spin Trapping Studies. DMPO, As₂O₃, cacodylic acid ((CH₃)₂AsOOH), and 80% H₂O₂ were all commercially obtained. Dimethylarsinous acid was prepared by allowing dimethyliodoarsine, (CH₃)₂AsI, to hydrolyze in solution. Dimethyliodoarsine was prepared by reduction of cacodylic acid following a previously established procedure⁶¹ and purity of the product was confirmed by GC/MS. All solutions for spin trapping were prepared using Dulbecco's phosphate buffered saline solution at pH 7.4. The total volume of each solution used for the EPR measurement was 50 μ L, and was loaded into a 50 μ L quartz micropipette. All samples contain 100 mM arsenite species concentration and 100 mM DMPO in aerobic PBS. Experimental conditions were as follows: DMPO and As₂O₃; DMPO, As₂O₃ and 0.2% H₂O₂;

DMPO, As₂O₃, 0.2% H₂O₂ and 3.5 mM Fe^{II}; DMPO, As₂O₃, and 3.5 mM Fe^{II}. Experiments were repeated with (CH₃)₂AsOH in place of arsenite. Negative controls used DMPO in pure PBS. Positive control used DMPO in the presence of H₂O₂ and irradiation with 254 nm light.

Results and Discussion

Spin trapping. Spin trapping with DMPO in aqueous solutions of trivalent arsenic yielded various spin adducts, however, no arsenic-centered radicals were detected in this way due to the absence of splitting pattern from ⁷⁵As with $I_{As} = 3/2$. Trivalent arsenic is a demonstrably powerful reducing agent and single electron transfers to ROS such as HO[•] have been demonstrated to be highly kinetically favorable.⁶²

Spin trapping of a solution containing DMA^{III}, H₂O₂, and in the presence or absence of Fe^{II} yielded an acylnitroxide adduct (Figure 1)⁶³ that is likely formed from the hydrolysis of superoxide (O₂^{•-}) or peroxy (HO₂[•]) radical adducts. Spin trapping of a solution containing DMA^{III} and Fe^{II} yielded predominantly HO^{•64} and C-centered adduct (Figure 2).⁶⁵ Spin trapping of a solution containing DMPO and DMA^{III} yielded HO[•] as the major species with minor species of alkyl radical adduct (Figure 3). Spin trapping of a solution containing As^{III}, H₂O₂, and Fe^{II} yielded predominantly HO[•] adduct and C-centered adduct, with open chain nitrone^{63,66} and HO₂[•] adduct as minor species (Figure 4). The presence of the open chain nitrone is suggested as the source of the carbon-centered adduct.⁶⁷ Spin trapping of a solution containing As^{III} and H₂O₂ yielded mostly HO[•] adduct, and also open chain nitrone and C-centered adduct (Figure 5). Spin trapping of a solution containing As^{III} and Fe^{II} yielded mostly HO[•] radical adduct and C-centered adduct, with minor products being open chain nitrone and HO₂[•] adduct (Figure 6). Spin trapping of a solution containing DMPO and As^{III} gave mostly HO[•], with a minor species of C-centered

adduct and possible open chain nitron (Figure 7). We found no evidence of adducts formed between the nitron and any As-containing radical compounds. We propose that the trapped ROS's were generated as byproducts of a rapid oxidation of trivalent to pentavalent arsenic.

The appearance of open-chain nitrones and C-centered adducts is proposed to be the result of reductive $\text{DMPO}^{\bullet}\text{-OOH}$ decomposition. This decomposition has been shown to occur *via* a ring-opening mechanism, leading to carbon-centered radicals.⁶⁶ Once formed, such radicals would be rapidly trapped. Decomposition analysis of adducts formed in a solution containing As^{III} , H_2O_2 , and Fe^{II} supports this hypothesis as $\text{O}_2^{\bullet-}$ adduct decomposes to form the open chain nitron (Figure 8). However, one would expect a proportionate formation of C-centered radical adduct with ring-opening, but an inverse relationship exists there too, with C-centered adduct being present in detectable quantity only for the first 200s of the experiment.

Theoretical Studies. Theoretical analysis of the electronic structures of various proposed As^{IV} radical intermediates was carried out at the PCM/B3LYP/6-31G**//B3LYP/6-31G* level of theory (Figure 7). For a more systematic model of the effect of methylation on arsenic toxicity, monomethyl arsenic species were included in the calculations. Trends in structure and reactivity were readily observed. The neutral tetravalent species (formed by one electron oxidation of the corresponding trivalent species *via* radical addition of hydroxyl radical to the As atom) exhibited a see-saw molecular geometry with methyl groups always located equatorially. An analysis of electron spin-density revealed the axial oxygen atoms to have greater spin density compared to the nonexistent spin on the equatorial oxygens (as in As^{III} and MMA^{III}). Additionally, increasing methylation character was proportional to an increase in spin density on the As atom. This may be explained by the increased As-OH axial bond lengths with methylation character caused by the bulky equatorial methyl groups and by the electron donating effect of the methyl groups. The

cationic tetravalent intermediates exhibited the same trend in increasing As spin density with increasing methyl substitution, although spin density is evenly distributed across the oxygen atoms arranged in a trigonal pyramidal molecular geometry.

We examined (at the same level of theory) the mechanisms of generation of the tetravalent arsenic radical intermediates and subsequent oxidation to the pentavalent arsenics with radical products including superoxide and hydroperoxyl radical. The mechanisms examined used common oxidants including O_2 , $O_2^{\cdot-}$, and H_2O_2/HO^{\cdot} which have been previously established as causal agents in the oxidation of As^{III} to As^V , with As^{IV} the proposed intermediate.⁶⁸ The mechanisms and results, shown in Tables 1-3, reveal an important trend: increasing methyl character of the starting trivalent arsenic species is proportional to increasing exoergicity of reaction. Thus, oxidation from trivalent to pentavalent arsenic and subsequent generation of reactive oxygen species byproducts is more energetically favorable with increasing methyl substitution.

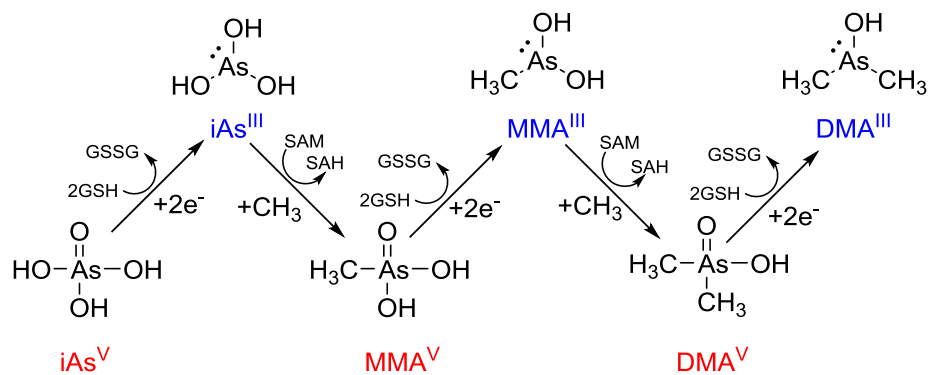
Increasing evidence^{16, 69-71} suggests that the organic trivalent arsenics are the most toxic of all common arsenic species. It has been proposed that this increased toxicity is due to the high membrane permeability of organic trivalent arsenics, with DMA^{III} being more permeable than MMA^{III} or As^{III} .^{72, 73} However recent studies present evidence that non-methylating urothelial cells are less susceptible to As^{III} exposure than methylating hepatocytes.⁷⁴ This is interesting because it means that the methylation occurs only after the inorganic arsenite has already permeated the membrane and is inside of the cell, suggesting that the increased toxicity of the methylated arsenites is due to its intrinsic toxic character rather than greater membrane permeability. Recent experiments have also shown that hepatocytes of catalase-knockout mice exposed to H_2O_2 or MMA^{III} exhibit significantly higher occurrences of DNA strand breaks than

in wild type mice with the intact gene for catalase (catalase catalyses the conversion of H_2O_2 to oxygen and water, thus limiting the production of damaging hydroxyl radical).⁷⁵ In the same study, EPR spin trapping with DMPO of the cell contents showed the presence of $\bullet\text{OH}$ in hepatocytes of mice exposed to H_2O_2 or MMA^{III} , the signal for which was greatly reduced in wild type mice versus catalase-knockout mice. This suggests that the genotoxic effects of organic arsenite exposure are mediated by ROS, in particular $\bullet\text{OH}$. In consideration of recent studies that link arsenic exposure to oxidative stress and ROS generation, we hold our study to be a timely and relevant contribution. Our findings show that arsenites generate various ROS when exposed to common oxidants in solution. Both H_2O_2 and O_2 have previously been demonstrated to oxidize As^{III} to As^{V} and DMA^{III} to DMA^{V} ,^{68, 76} and our theoretical calculations suggesting a basis for the increased redox activity of methylated arsenites can be applied to the observed trends in arsenic methylation and toxicity. That methylation appears to localize electron spin density on arsenic centered radicals may explain the increasing exoergicity of radical oxidation proportional to increasing methyl substitution of arsenite. In turn the increasing exoergicity of methylated arsenites oxidation in water and thus increasing ROS production may help to explain the trends in arsenic toxicity. Of additional interest is the application of inorganic arsenite as an effective chemotherapeutic agent in the treatment of acute promyelocytic leukemia,^{20, 22} which may seem counterintuitive as arsenite is known to be a potent human carcinogen. However, evidence suggests that the dose-response relationship induced by arsenic exposure is not linear, rather it is biphasic. Thus at low concentrations arsenite acts as a carcinogen, causing tumorigenesis by stimulating transcription factors that express genes promoting cell proliferation and malignant transformation and causing apoptosis at higher concentrations.^{77, 78} However, at higher concentrations arsenic acts to promote apoptosis by causing genomic instability.^{79, 80} More recent

evidence pinpoints at least one biphasic mechanism by which arsenic acts to promote and suppress proliferation with increasing concentrations: in human keratinocytes exposed to low levels of arsenite, there is inactivation of the tumor suppressor protein p53 (an inhibitor of survivin) and correspondingly heightened levels of survivin (mediator of apoptosis resistance, highly expressed in cancer cells) while higher concentrations sees the opposite effect: high activation of p53 and negative regulation of survivin.⁸¹ However, it must be noted that these studies cannot pinpoint the exact species (or multiples species) of arsenic (be it inorganic or biomethylated, tri- or penta- valent) responsible for these effects. For example, the urine of acute promyelocytic leukemia patients treated with inorganic arsenite has been found to contain considerable levels of methylated arsenic.⁸²

Another study compared gene expression and cell viability between iAs^{III} , MMA^{III} , and DMA^{III} in human keratinocytes.⁸³ After analyzing trends in cell proliferation, apoptosis, and the expression of genes promoting cellular oxidative defense, apoptosis factors and growth factors, the study's authors concluded that MMA^{III} was the most cytotoxic species ($LC_{50} = 2.8\mu M$), followed by DMA^{III} ($LC_{50} = 5.6\mu M$), and then iAs^{III} ($LC_{50} = 17\mu M$). In human bladder cancer cells, treatment with DMA^{III} or $DMMTA^V$ (dimethylmonothioarsinic acid) drastically reduced GSH and p53 levels compared to control cells, while iAs also decreased p53 it was not as drastic as DMA^{III} and treatment actually increased GSH levels compared to control.¹⁵ One should not compare these results with the previously described study in human keratinocytes as the cancer cells have already demonstrated a compromised oncosuppressive system so further toxic insult is not likely to produce the response seen in normal cells exposed to high levels of arsenic. The Authors of this study suggest that the increased toxicity of the organic arsenicals was occurring *via* a cycle of GSH depletion from catalyzed reduction of DMA^V to DMA^{III} and subsequent

regeneration of the trivalent form. Our theoretical results corroborate this finding, we found the oxidation of DMA^{III} to DMA^{V} to be highly exoergic in multiple redox pathways. Our results also suggest a similar ROS speciation between iAs^{III} and DMA^{III} , with no difference in signal intensity (as would be expected from our calculations, the oxidation from tri to pentavalent arsenical is highly exoergic for both species).



Scheme 1. Biomethylation of arsenic in humans. The reduction steps are catalyzed by As^V reductase, the oxidative methylation steps are catalyzed by As^{III} methyltransferase, with S -adenosyl methionine (SAM) as the methyl donor demethylated to S -adenosyl-L-homocysteine (SAH). Reduced glutathione (GSH) serves as the electron donor.¹⁷

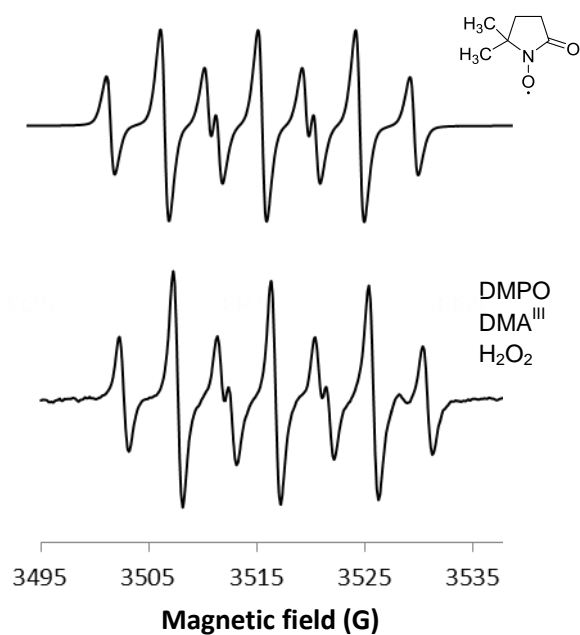


Figure 1. Simulated (top) and experimental (bottom) EPR spectrum of a solution containing DMPO, DMA^{III}, and H₂O₂ showing a spectral profile and splitting parameters characteristic of the oxidized DMPO radical adduct DMPOX: $a_N = 9.1\text{G}$, $a_{\beta\text{-H}} = 5.1\text{G}$, $a_{\gamma\text{-H}} = 5.0\text{G}$.

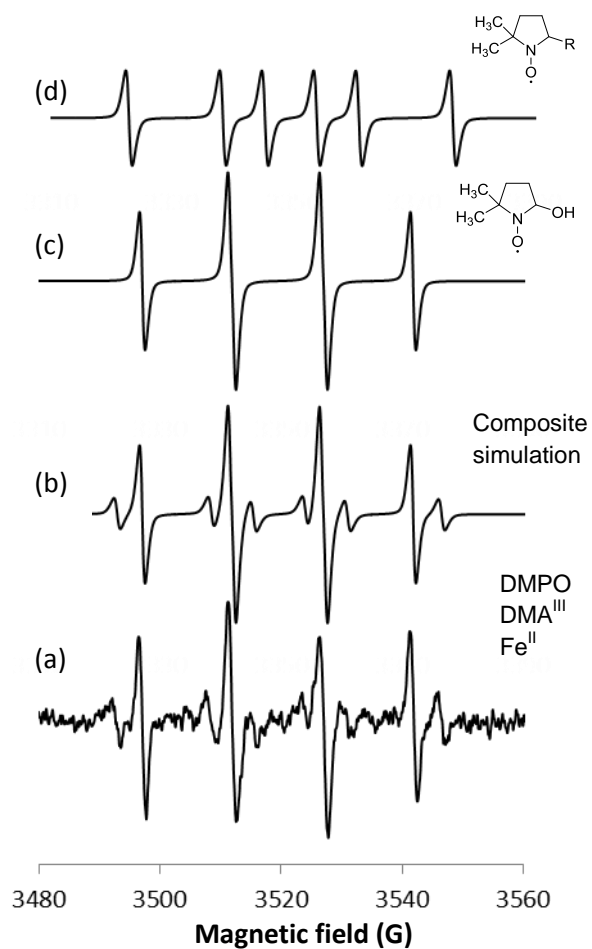


Figure 2. (a) Experimental and (b) simulated EPR spectrum of a solution containing DMPO, DMA^{III}, and Fe^{II}. Simulation of the spectrum components (c) hydroxyl radical adduct (76.4%): $a_N = 15.1$ G, $a_{\beta-H} = 14.5$ G; (d) alkyl radical adduct (23.6%): $a_N = 15.5$ G, $a_{\beta-H} = 22.5$ G.

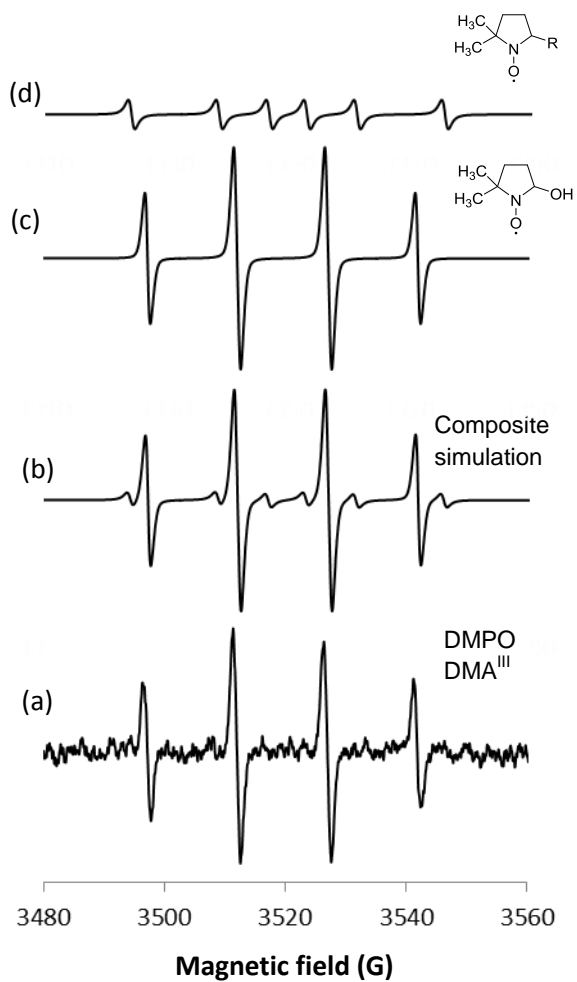


Figure 3. (a) Experimental and (b) simulated EPR spectrum of a solution containing DMPO and DMA^{III}. Simulation of the spectrum components (c) hydroxyl radical adduct (81.6%): $a_N = 15.0$ G, $a_{\beta-H} = 14.5$ G; (d) alkyl radical adduct (18.4%): $a_N = 14.5$ G, $a_{\beta-H} = 22.8$ G.

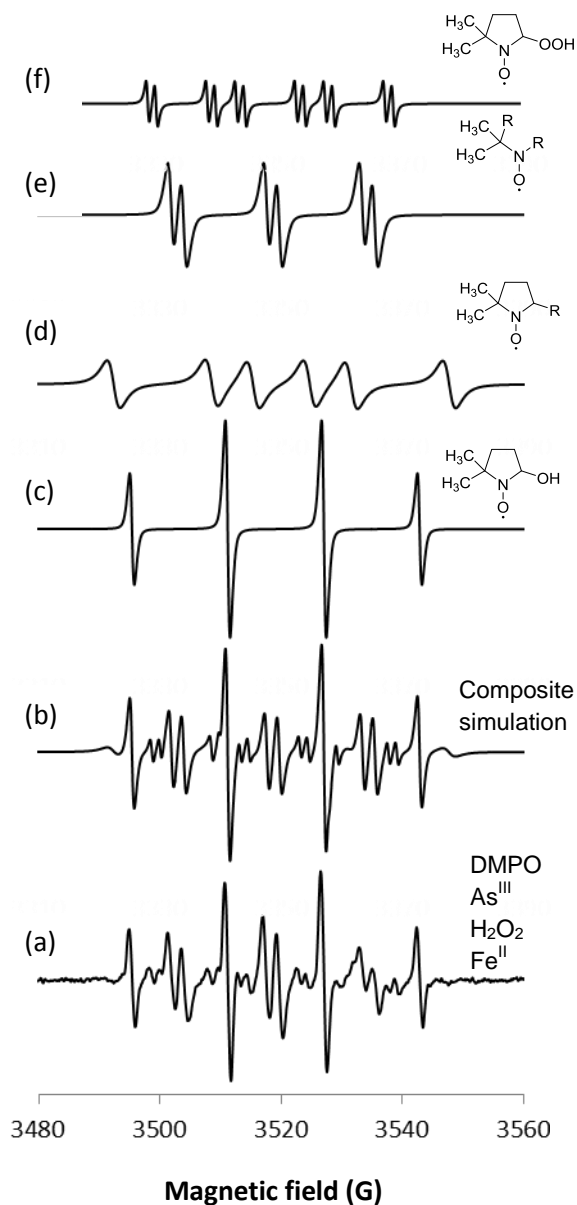


Figure 4. (a) Experimental and (b) simulated EPR spectrum of a solution containing DMPO, As^{III} , H_2O_2 , and Fe^{II} . Simulation of the spectrum components (c) hydroxyl radical adduct (32.2%): $a_N = 15.9$ G, $a_{\beta-H} = 15.7$ G; (d) alkyl radical adduct (27.5%): $a_N = 16.2$ G, $a_{\beta-H} = 23.0$ G; (e) open chain-nitron (30.6%): $a_N = 15.8$ G, $a_{\beta-H} = 2.1$ G; (f) hydroperoxyl radical adduct (9.7%): $a_N = 14.6$ G, $a_{\beta-H} = 9.8$ G, $a_{\gamma-H} = 1.4$ G.

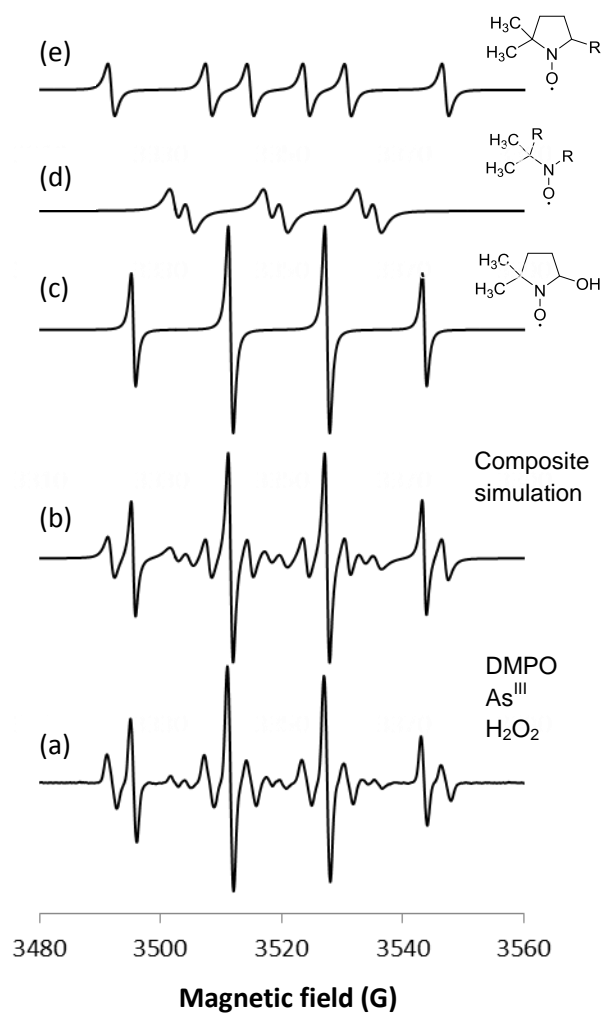


Figure 5. (a) Experimental and (b) simulated EPR spectrum of a solution containing DMPO, As^{III} , and H_2O_2 . Simulation of the spectrum components (c) hydroxyl radical adduct (37.5%): $a_{\text{N}} = 15.9$ G, $a_{\beta\text{-H}} = 16.2$ G; (d) open chain-nitron (31.6%): $a_{\text{N}} = 15.5$ G, $a_{\beta\text{-H}} = 2.5$ G; (e) alkyl radical adduct (30.9%): $a_{\text{N}} = 16.1$ G, $a_{\beta\text{-H}} = 22.9$ G.

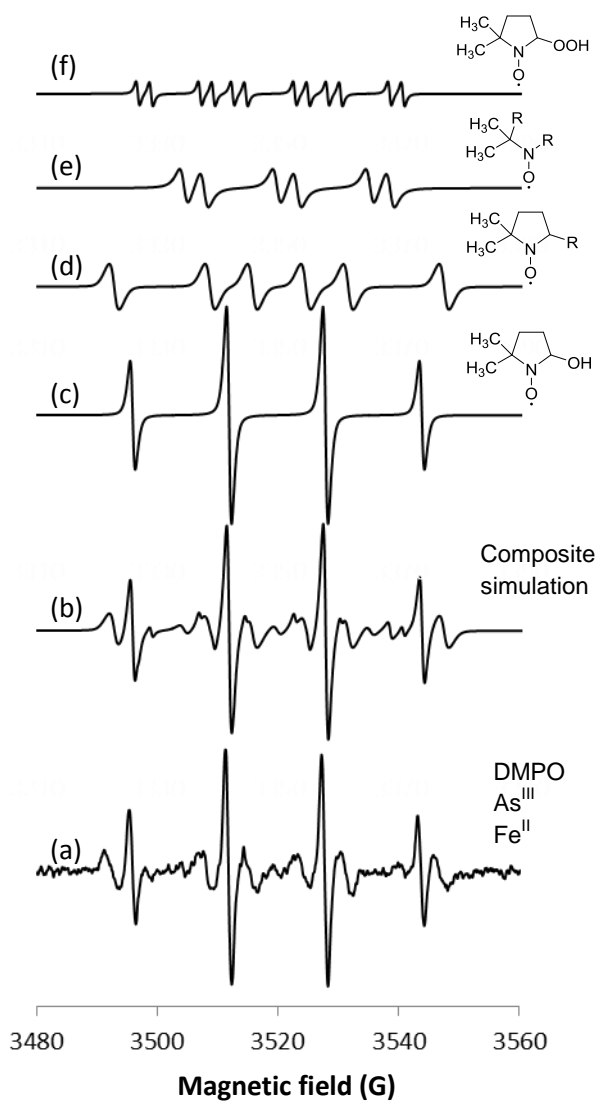


Figure 6. (a) Experimental and (b) simulated EPR spectrum of DMPO, As^{III} , and Fe^{II} in aqueous solution. Simulation of the spectrum components (c) hydroxyl radical adduct (44.3%): $a_{\text{N}} = 15.9$ G, $a_{\beta\text{-H}} = 15.9$ G; (d) alkyl radical adduct (37.4%) : $a_{\text{N}} = 15.8$ G, $a_{\beta\text{-H}} = 22.8$ G; (e) open chain-nitron (13.3%): $a_{\text{N}} = 15.4$ G, $a_{\beta\text{-H}} = 3.4$ G; (f) hydroperoxyl radical adduct (5.0%): $a_{\text{N}} = 15.6$ G, $a_{\beta\text{-H}} = 10.3$ G, $a_{\gamma\text{-H}} = 2.2$ G.

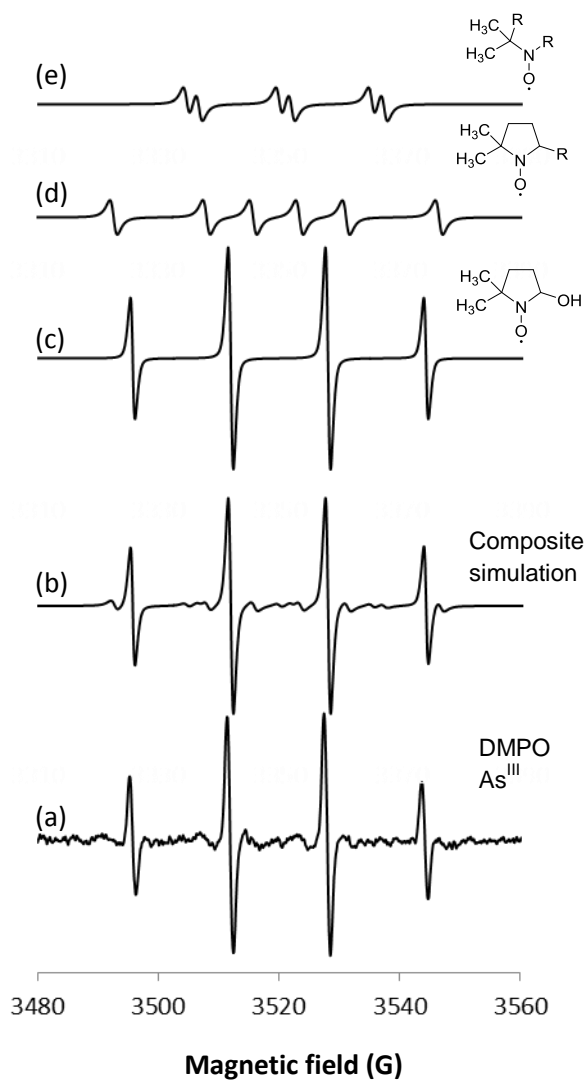


Figure 7. (a) Experimental and (b) simulated EPR spectrum of DMPO and As^{III} in aqueous solution. Simulation of the spectrum components (c) hydroxyl radical adduct (72.4%): $a_{\text{N}} = 16.0$ G, $a_{\beta\text{-H}} = 16.2$ G; (d) alkyl radical adduct (20.4%): $a_{\text{N}} = 15.4$ G, $a_{\beta\text{-H}} = 23.1$ G; (e) open chain-nitron (7.2%): $a_{\text{N}} = 15.3$ G, $a_{\beta\text{-H}} = 2.8$ G.

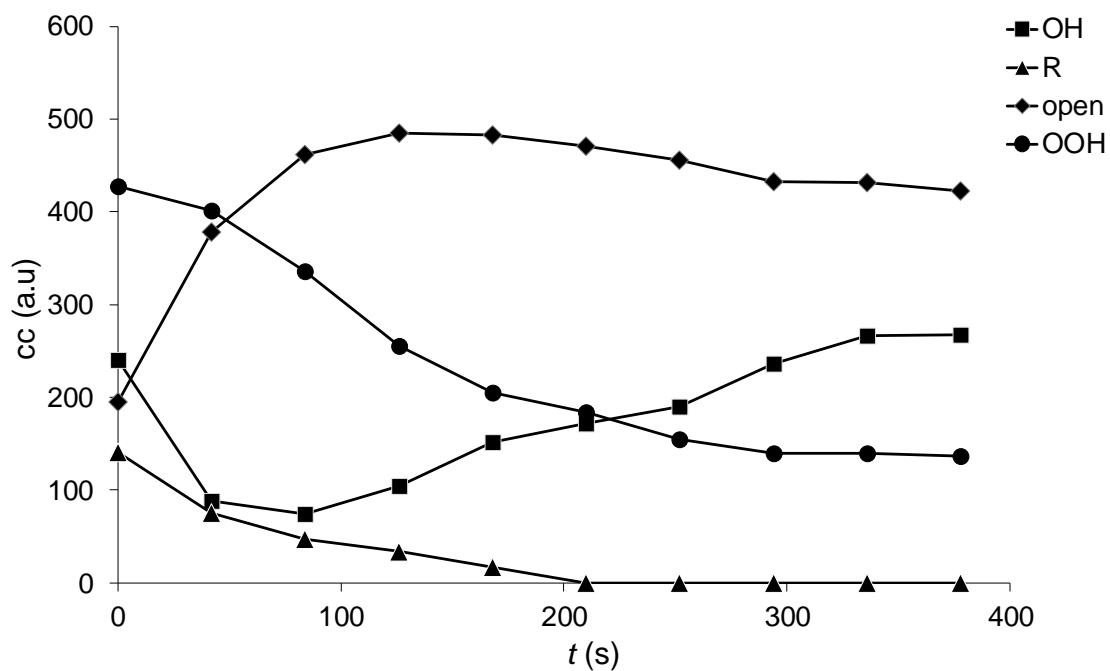


Figure 8. Decomposition of the various radical adducts in a solution containing DMPO, As^{III} , H_2O_2 , and Fe^{II} . Notice the decomposition of DMPO \cdot -OOH adduct in relationship to formation of the open-chain nitrene.

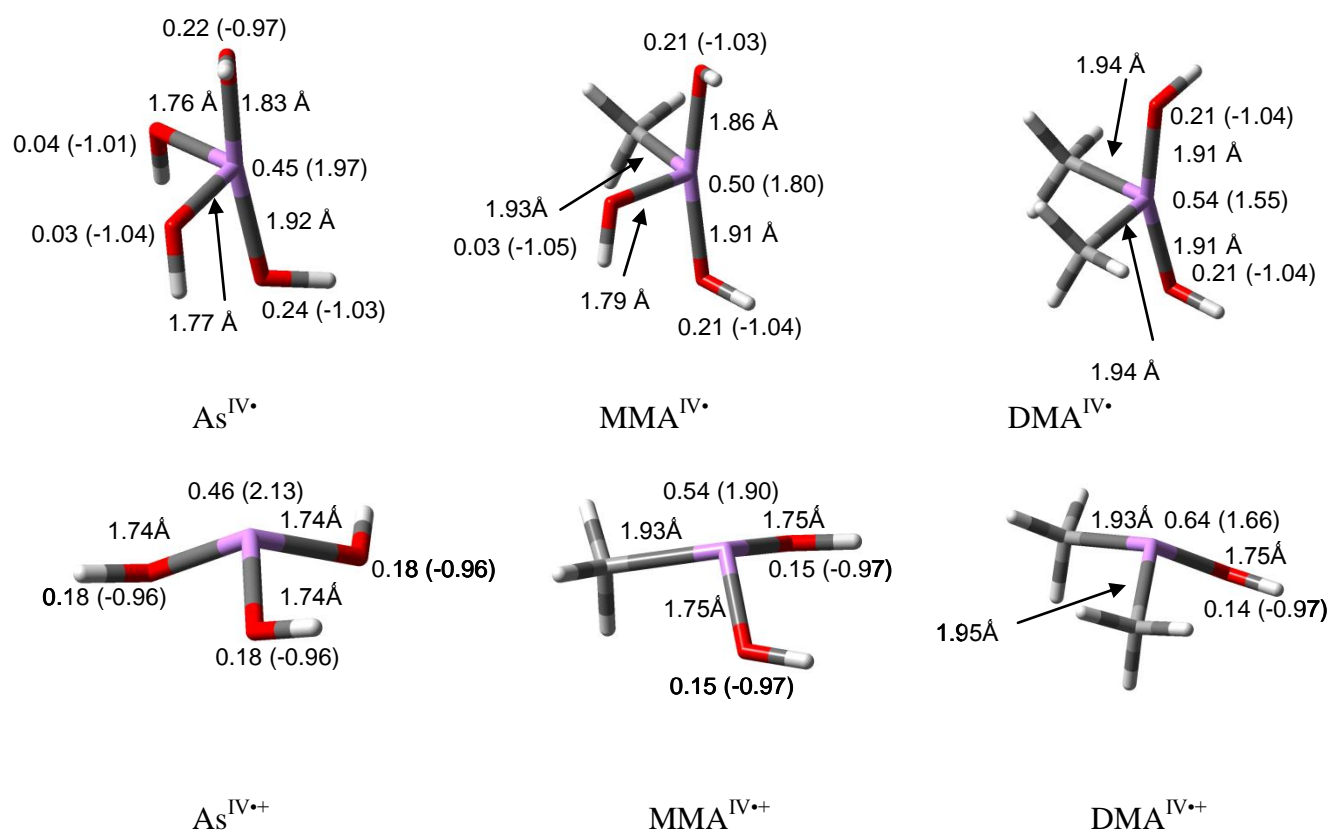


Figure 7. Aqueous phase bond distances, spin and charge (in parentheses) densities of various radicals at the PCM/B3LYP/6-31+G**//B3LYP/6-31G* level. Note the trend of increasing spin density on the As atom with increasing methyl substitution. Also note the absence of spin density on the equatorial oxygen atoms on the seesaw geometries of As^{IV^\bullet} and MMA^{IV^\bullet} .

Table 1. Free energies (in kcal/mol) of hydroxyl radical-initiated radical oxidation of arsenites at the PCM/B3LYP/6-31G**//B3LYP/6-31G* level of theory.

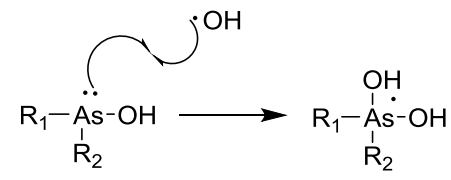
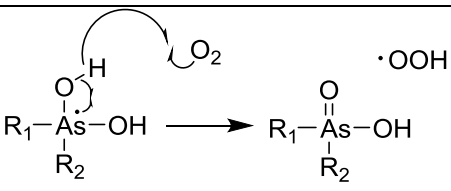
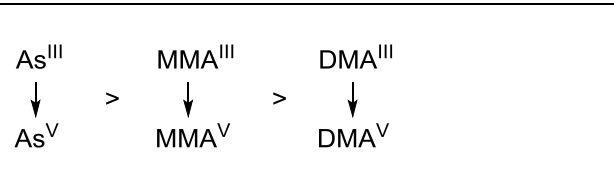
	R₁, R₂	ΔG_{298K, I}
	OH, OH	-14.8
	OH, Me	-20.0
	Me, Me	-23.2
	R₁, R₂	ΔG_{298K, II}
	OH, OH	-10.7
	OH, Me	-16.7
	Me, Me	-18.9
		ΔG_{298K, I + II}
		-25.5
		-36.7
		-42.1

Table 2. Free energies (in kcal/mol) of superoxide-initiated radical oxidation of arsenites at the PCM/B3LYP/6-31G**//B3LYP/6-31G* level of theory.

	R₁, R₂	$\Delta G_{298K, I}$
	OH, OH	25.4
	OH, Me	8.4
	Me, Me	-3.1
	R₁, R₂	$\Delta G_{298K, II}$
	OH, OH	-62.1
	OH, Me	-50.3
	Me, Me	-42.0
	R₁, R₂	$\Delta G_{298K, III}$
	OH, OH	-10.7
	OH, Me	-16.7
	Me, Me	-18.9
	$\Delta G_{298K, I + II + III}$	
	-47.4	
	-58.6	
	-64.0	

Table 3. Free energies (in kcal/mol) of oxygen-initiated radical oxidation of arsenites at the PCM/B3LYP/6-31G**//B3LYP/6-31G* level of theory.

	R₁, R₂	$\Delta G_{298K, I}$
	OH, OH	81.4
	OH, Me	64.4
	Me, Me	52.9
	R₁, R₂	$\Delta G_{298K, II}$
	OH, OH	-62.1
	OH, Me	-50.3
	Me, Me	-41.9
	R₁, R₂	$\Delta G_{298K, III}$
	OH, OH	-10.7
	OH, Me	-16.7
	Me, Me	-18.9
	$\Delta G_{298K, I + II + III}$	
	8.6	
	-2.6	
	-7.9	

References

- (1) Chen, C. J., Chuang, Y. C., Lin, T. M., and Wu, H. Y. (1985) Malignant neoplasms among residents of a blackfoot disease-endemic area in Taiwan: high arsenic artesian well water and cancers. *Cancer Res.*, *45*, 5895-5899.
- (2) Chen, C. J., Kuo, T. L., and Wu, M. M. (1988) Arsenic and cancers. *Lancet*, *1*, 414-415.
- (3) Morales, K. H., Ryan, L., Kuo, T. L., Wu, M. M., and Chen, C. J. (2000) Risk of internal cancers from arsenic in drinking water. *Environ. Health Perspect.*, *108*, 655-661.
- (4) Smith, A. H., Hopenhayn-Rich, C., Bates, M. N., Goeden, H. M., Hertz-Picciotto, I., Duggan, H. M., Wood, R., Kosnett, M. J., and Smith, M. T. (1992) Cancer risks from arsenic in drinking water. *Environ. Health Perspect.*, *97*, 259-267.
- (5) Shi, H., Shi, X., and Liu, K. J. (2004) Oxidative mechanism of arsenic toxicity and carcinogenesis. *Mol. Cell. Biochem.*, *255*, 67-68.
- (6) Ng, J. C., Wang, J., and Shraim, A. (2003) A global health problem caused by arsenic from natural sources. *Chemosphere*, *52*, 1353-1359.
- (7) Tseng, W. P. (1977) Effects and dose--response relationships of skin cancer and blackfoot disease with arsenic. *Environ. Health Perspect.*, *19*, 109-119.
- (8) Hsueh, Y. M., Cheng, G. S., Wu, M. M., Yu, H. S., Kuo, T. L., and Chen, C. J. (1995) Multiple risk factors associated with arsenic-induced skin cancer: effects of chronic liver disease and malnutritional status. *Br. J. Cancer*, *71*, 109-114.
- (9) Buratti, M., Calzaferri, G., Caravelli, G., Colombi, A., Maroni, M., and Foa, V. (1984) Significance of arsenic metabolic forums in urine. Part I: Chemical speciation. *Int. J. Environ. Anal. Chem.*, *17*, 25-34.
- (10) Lindgren, A., Danielsson, B. R., Dencker, L., and Vahter, M. (1984) Embryotoxicity of arsenite and arsenate: distribution in pregnant mice and monkeys and effects on embryonic cells in vitro. *Acta. Pharmacol. Toxicol. (Copenh)*. *54*, 311-320.
- (11) Zakharyan, R. A., Sampayo-Reyes, A., Healy, S. M., Tsaprailis, G., Board, P. G., Liebler, D. C., and Aposhian, H. V. (2001) Human monomethylarsonic acid (MMA(V)) reductase is a member of the glutathione-S-transferase superfamily. *Chem. Res. Toxicol.*, *14*, 1051-1057.
- (12) Radabaugh, T. R., Sampayo-Reyes, A., Zakharyan, R. A., and Aposhian, H. V. (2002) Arsenate reductase II. Purine nucleoside phosphorylase in the presence of dihydrolipoic acid is a route for reduction of arsenate to arsenite in mammalian systems *Chem. Res. Toxicol.*, *15*, 692-698.

- (13) Kligerman, A. D., Doerr, C. L., Tennant, A. H., Harrington-Brock, K., Allen, J. W., Winkfield, E., Poorman-Allen, P., Kundu, B., Funasaka, K., Roop, B. C., Mass, M. J., and DeMarini, D. M. (2003) Methylated trivalent arsenicals as candidate ultimate genotoxic forms of arsenic: induction of chromosomal mutations but not gene mutations. *Environ. Mol. Mutagen.*, *42*, 192-205.
- (14) Morel, G., Cluet, J. L., Telolahy, P., Yang, H. M., Thieffry, N., and de Ceaurriz, J. (1995) Interindividual variability in the urinary excretion of inorganic arsenic metabolites by C57 BL/6J mice: possible involvement of a thiol/disulfide exchange mechanism. *Toxicol. Lett.*, *78*, 111-117.
- (15) Naranmandura, H., Carew, M. W., Xu, S., Lee, J., Leslie, E. M., Weinfeld, M., and Le, X. C. (2011) Comparative toxicity of arsenic metabolites in human bladder cancer EJ-1 cells. *Chem. Res. Toxicol.*, *24*, 1586-1596.
- (16) Petrick, J. S., Ayala-Fierro, F., Cullen, W. R., Carter, D. E., and Vasken Aposhian, H. (2000) Monomethylarsonous acid (MMA(III)) is more toxic than arsenite in Chang human hepatocytes. *Toxicol. Appl. Pharmacol.*, *163*, 203-207.
- (17) Styblo, M., Drobna, Z., Jaspers, I., Lin, S., and Thomas, D. J. (2002) The role of biomethylation in toxicity and carcinogenicity of arsenic: a research update. *Environ. Health Perspect.*, *110*, 767-771.
- (18) Hernandez, A., Xamena, N., Surralles, J., Sekaran, C., Tokunaga, H., Quinteros, D., Creus, A., and Marcos, R. (2008) Role of the Met(287) Thr polymorphism in the AS3MT gene on the metabolic arsenic profile. *Mutat. Res.*, *637*, 80-92.
- (19) Vahter, M., and Concha, G. (2001) Role of metabolism in arsenic toxicity. *Pharmacol. Toxicol.*, *89*, 1-5.
- (20) Soignet, S. L., Maslak, P., Wang, Z. G., Jhanwar, S., Calleja, E., Dardashti, L. J., Corso, D., DeBlasio, A., Gabrilove, J., Schienberg, D. A., and Pandolfi, P. P. (1998) Complete remission after treatment of acute promyelocytic leukemia with arsenic trioxide. *N. Engl. J. Med.*, *339*, 1341-1348.
- (21) Lazo, G., Kantarjian, H., Estey, E., Thomas, D., O'Brien, S., and Cortes, J. (2003) Use of arsenic trioxide (As₂O₃) in the treatment of patients with acute promyelocytic leukemia: the M. D. Anderson experience
Cancer, *97*, 2218-2224.
- (22) Soignet, S. L., Frankel, S. R., Douer, D., Tallman, M. S., Kantarjian, H., Calleja, E., Stone, R. M., Kalaycio, M., Schienberg, D. A., Steinherz, P., Sievers, E. L., Coutre, S., Dahlberg, S., Ellison, R., and Warrel, R. P. J. (2001) United States multicenter study of arsenic trioxide in relapsed acute promyelocytic leukemia. *J. Clin. Oncol.*, *19*, 3852-3860.
- (23) Shen, Z. X., Shi, Z. Z., Fang, J., Gu, B. W., Li, J. M., Zhu, Y. M., Shi, J. Y., Zheng, P. Z., Yan, H., Liu, Y. F., Chen, Y., Shen, Y., Wu, W., Tang, W., Waxman, S., De The, H.,

- Wang, Z. Y., Chen, S. J., and Chen, Z. (2004) All-trans retinoic acid/As₂O₃ combination yields a high quality remission and survival in newly diagnosed acute promyelocytic leukemia *Proc. Natl. Acad. Sci. U S A*
- (24) Fox, E., Razzouk, B. I., Widemann, B. C., Xiao, S., O'Brien, M., Goodspeed, W., Reaman, G. H., Blaney, S. M., Murgo, A. J., Balis, F. M., and Adamson, P. C. (2008) Phase 1 trial and pharmacokinetic study of arsenic trioxide in children and adolescents with refractory or relapsed acute leukemia, including promyelocytic leukemia or lymphoma. *Blood*, *111*, 566-573.
- (25) Chen, Y. C., Lin-Shiau, S. Y., and Lin, L. K. (1998) Involvement of reactive oxygen species and caspase 3 activation in arsenite-induced apoptosis. *J. Cell. Physiol.*, *177*, 324-333.
- (26) Hei, T. K., Liu, S. X., and Waldren, C. (1998) Mutagenicity of arsenic in mammalian cells: role of reactive oxygen species. *Proc. Natl. Acad. Sci. U S A*, *95*, 8103-8107.
- (27) Jomova, K., Jenisova, Z., Feszterova, M., Baros, S., Liska, J., Hudecova, D., Rhodes, C. J., and Valko, M. (2011) Arsenic: toxicity, oxidative stress and human disease. *J. Appl. Toxicol.*, *31*, 95-107.
- (28) Liu, S. X., Athar, M., Lippai, I., Waldren, C., and Hei, T. K. (2001) Induction of oxyradicals by arsenic: implication for mechanism of genotoxicity *Proc. Natl. Acad. Sci. U S A*, *98*, 1643-1648.
- (29) Pelicano, H., Feng, L., Zhou, Y., Carew, J. S., Hileman, E. O., Plunkett, W., Keating, M. J., and Huang, P. (2003) Inhibition of mitochondrial respiration: a novel strategy to enhance drug-induced apoptosis in human leukemia cells by a reactive oxygen species-mediated mechanism *J. Biol. Chem.*, *278*, 37832-37839.
- (30) Wang, T. S., Kuo, C. L., Jan, K. Y., and Huang, H. (1996) Arsenite induces apoptosis in Chinese hamster ovary cells by generation of reactive oxygen species. *J. Cell. Physiol.*, *169*, 256-268.
- (31) Shi, H., Hudson, L. G., and Liu, K. J. (2004) Oxidative stress and apoptosis in metal ion-induced carcinogenesis *Free Radic. Biol. Med.*, *37*, 582-593.
- (32) Lu, J., Chew, E.-H., and Holmgren, A. (2007) Targeting thioredoxin reductase is a basis for cancer therapy by arsenic trioxide. *Proc. Natl. Acad. Sci. U S A*, *104*, 12288-12293.
- (33) Cheng, X., Quintas-Cardama, A., Golemovic, M., Zingaro, R., Gao, M. Z., Freireich, E. J., Andreeff, M., Kantarjian, H. M., and Verstovsek, S. (2012) The organic arsenic derivative GMZ27 induces PML-RAR α -independent apoptosis in myeloid leukemia cells. *Anticancer Res.*, *32*, 2871-2880.
- (34) Selvaraj, V., Armistead, M. Y., Cohenford, M., and Murray, E. (2013) Arsenic trioxide (As₂O₃) induces apoptosis and necrosis mediated cell death through mitochondrial

- membrane potential damage and elevated production of reactive oxygen species in PLHC-1 fish cell line. *Chemosphere*, *90*, 1201-1209.
- (35) Thomas-Schoemann, A., Batteux, F., Mongaret, C., Nicco, C., Chereau, C., Annereau, M., Dauphin, A., Goldwasser, F., Weill, B., Lemare, F., and Alexandre, J. (2012) Arsenic trioxide exerts antitumor activity through regulatory T cell depletion mediated by oxidative stress in a murine model of colon cancer. *J. Immunol.*, *189*, 5171-5177.
- (36) Nesnow, S., Roop, B. C., Lambert, G., Kadiiska, M. B., Mason, R. P., Cullen, W. R., and Mass, M. J. (2002) DNA damage induced by methylated trivalent arsenicals is mediated by reactive oxygen species. *Chem. Res. Toxicol.*, *15*.
- (37) Kojima, C., Ramirez, D. C., Tokar, E. J., Himeno, S., Drobna, Z., Styblo, M., Mason, R. P., and Waalkes, M. P. (2009) Requirement of arsenic biomethylation for oxidative DNA damage. *J. Natl. Cancer Inst.*, *101*, 1670-1681.
- (38) Frisch, M. J., Trucks, G. W., Schlegel, H. B., Scuseria, G. E., Robb, M. A., Cheeseman, J. R., Scalmani, G., Barone, V., Mennucci, B., Peterson, G. A., Nakatsuji, H., Caricato, M., Li, X., Hratchian, H. P., Izamylov, A. F., Bloino, J., Zheng, G., Sonnenberg, J. L., Hada, M., Ehara, M., Toyota, K., Fukuda, R., Hasewaga, J., Ishida, M., Nakajima, T., Honda, Y., Kitao, O., Nakai, H., Vreven, T., Montgomery, J. A., Jr., Peralta, J. E., Ogliaro, F., Bearpark, M., Heyd, J. J., Brothers, E., Kudin, K. N., Staroverov, V. N., Kobayashi, R., Normand, J., Raghavachari, K., Rendell, A., Burant, J. C., Iyengar, S. S., Tomasi, J., Cossi, M., Rega, N., Millam, J. M., Klene, M., Knox, J. E., Cross, J. B., Bakken, V., Adamo, C., Jaramillo, J., Gomperts, R., Stratman, R. E., Yazyev, O., Austin, A. J., Cammi, R., Pomelli, C., Ochterski, J. W., Martin, R. L., Morokuma, K., Zakrzewski, V. G., Voth, G. A., Salvador, P., Dannenberg, J. J., Dapprich, S., Daniels, A. D., Farkas, O., Foresman, J. B., Ortiz, J. V., Ciolowski, J., and Fox, D. J. (2009) Gaussian 09.
- (39) Labanowski, J. W., and Andzelm, J. (1991) *Density Functional Methods in Chemistry*. Springer, New York.
- (40) Parr, R. G., and Yang, W. (1989) *Density Functional Theory in Atoms and Molecules*. Oxford University Press, New York.
- (41) Becke, A. D. (1988) Density-functional exchange-energy approximation with correct asymptotic behavior. *Phys. Rev. A*, *38*, 3098-3100.
- (42) Lee, C., Yang, W., and Parr, R. G. (1988) Development of the Colle-Salvetti correlation-energy formula into a functional of the electron density. *Phys. Rev. B Condens. Matter*, *37*, 785-789.
- (43) Becke, A. D. (1993) A new mixing of Hartree-Fock and local density-functional theories. *J. Chem. Phys.*, *98*, 1372.
- (44) Hehre, W. J., Radom, L., Schleyer, P. V., and Pople, J. A. (1986) *Ab Initio Molecular Orbital Theory*. John Wiley & Sons, New York.

- (45) Reed, A. E., Curtiss, L. A., and Weinhold, F. (1988) Intermolecular interactions from a natural bond orbital, donor-acceptor viewpoint. *Chem. Rev.*, 88, 899.
- (46) Tomasi, J., and Persico, M. (1994) Molecular interactions in solution: an overview of methods based on continuous distributions of the solvent. *Chem. Rev.*, 94, 2027-2094.
- (47) Cossi, M., Barone, V., Cammi, R., and Tomasi, J. (1996) Ab initio study of solvated molecules: a new implementation of the polarizable continuum model. *Chem. Phys. Lett.*, 255, 327-335.
- (48) Barone, V., Cossi, M., and Tomasi, J. (1997) A new definition of cavities for the computation of solvation free energies by the polarizable continuum model. *J. Chem. Phys.*, 107, 3210.
- (49) Barone, V., Cossi, M., and Tomasi, J. (1998) Geometry optimization of molecular structures in solution by the polarizable continuum model. *J. Comput. Chem.*, 19, 404-417.
- (50) Tomasi, J., Mennucci, B., and Cammi, R. (2005) Quantum mechanical continuum solvation models. *Chem. Rev.*, 105, 2999-3094.
- (51) Tarroni, R., and Clouthier, D. J. (2009) Heavy atom nitroxyl radicals. I: An *ab initio* study of the ground and lower electronic excited states of the H₂As=O free radical. *J. Chem. Phys.*, 131, 114310.
- (52) Rassolov, V. A., Ratner, M. A., Pople, J. A., Redfern, P. C., and Curtiss, L. A. (2001) 6-31G* basis set for third-row atoms. *J. Comput. Chem.*, 22, 976-984.
- (53) Scott, A. P., and Radom, L. (1996) Harmonic vibrational frequencies: An evaluation of hartree-fock, møller-plesset, quadratic configuration interaction, density functional theory, and semiempirical scale factors. *J. Phys. Chem.*, 100, 16502.
- (54) Cirujeda, J., Vidal-Gancedo, J., Jurgens, O., Mota, F., Novoa, J. J., Rovira, C., and Veciana, J. (2000) Spin density distribution of α -nitronyl aminoxyl radicals from experimental and ab Initio calculated ESR isotropic hyperfine coupling constants. *J. Am. Chem. Soc.*, 122.
- (55) Pavone, M., Cimino, P., De Angelis, F., and Barone, V. (2006) Interplay of stereoelectronic and enviromental effects in tuning the structural and magnetic properties of a prototypical spin probe: further insights from a first principle dynamical approach. *J. Am. Chem. Soc.*, 128, 4338.
- (56) Saracino, G. A. A., Tedeschi, A., D'Errico, G., Improta, R., Franco, L., Ruzzi, M., Corvaia, C., and Barone, V. (2002) Solvent polarity and pH effects on the magnetic properties of ionizable nitroxide radicals: A combined computational and experimental study of 2,2,5,5-tetramethyl-3-carboxypyrrolidine and 2,2,6,6-tetramethyl-4-carboxypiperidine nitroxides. *J. Phys. Chem. A*, 106, 10700-10706.

- (57) Barone, V. (1995) In *Recent Advances in Density Functional Theory, Part 1* (Cong, D. P., Ed.) p 287, World Scientific Publishing Co., Singapore.
- (58) Woon, D. E., and Dunning, T. H. (1995) Gaussian basis sets for use in correlated molecular calculations. V. Core-valence basis sets for boron through neon. *J. Chem. Phys.*, *103*, 4572.
- (59) Villamena, F. A., Merle, J. K., Hadad, C. M., and Zweier, J. L. (2005) Superoxide radical anion adduct of 5,5-dimethyl-1-pyrroline N-oxide (DMPO). 2. The thermodynamics of decay and EPR spectral properties. *J. Phys. Chem. A*, *109*, 6089.
- (60) Rockenbauer, A., and Korecz, L. (1996) Automatic computer simulations of ESR spectra. *Appl. Magn. Reson.*, *10*, 29–43.
- (61) Burrows, G. J., and Turner, E. E. (1920) CXLIX. - A new type of compound containing arsenic. *J. Chem. Soc., Trans.*, *117*, 1373-1383.
- (62) Buxton, G. V., Greenstock, C. L., Helman, W. P., and Ross, A. B. (1988) Critical review of rate constants for reactions of hydrated electrons, hydrogen atoms and hydroxyl radicals ($\bullet\text{OH}/\bullet\text{O}^-$ in aqueous solution. *J. Phys. Chem. Ref. Data*, *17*, 513.
- (63) Villamena, F. A. (2009) Superoxide radical anion adduct of 5,5-Dimethyl-1-pyrroline N-oxide. 5. Thermodynamics and kinetics of unimolecular decomposition. *J. Phys. Chem. A.*, *113*, 6398-6403.
- (64) Villamena, F. A., Hadad, C. M., and Zweier, J. L. (2004) Theoretical study of the spin trapping of hydroxyl radical by cyclic nitrones: a density functional theory approach. *J. Am. Chem. Soc.*, *126*, 1816-1829.
- (65) Rota, C., Barr, D. P., Martin, M. V., Guengerich, F. P., Tomasi, A., and Mason, R. P. (1997) Detection of free radicals produced from the reaction of cytochrome P-450 with linoleic acid hydroperoxide. *Biochem. J.*, *328*, 565-571.
- (66) Villamena, F. A. (2010) Superoxide radical anion adduct of 5,5-Dimethyl-1-pyrroline N-oxide. 6. Redox properties. *J. Phys. Chem. A.*, *114*, 1153-1160.
- (67) Guo, Q., Qian, S. Y., and Mason, R. P. (2003) Separation and identification of DMPO adducts of oxygen-centered radicals formed from organic hydroperoxides by HPLC-ESR, ESI-MS and MS/MS. *J. Am. Mass. Spectrom.*, *14*, 862-871.
- (68) Lee, H., and Choi, W. (2002) Photocatalytic oxidation of arsenite in TiO_2 suspension: kinetics and mechanisms. *Environ. Sci. Technol.*, *36*, 3872-3878.
- (69) Styblo, M., Del Razo, L. M., Vega, L., Germolec, D. R., LeCluyse, E. L., Hamilton, G. A., Reed, W., Wang, C., Cullen, W. R., and Thomas, D. J. (2000) Comparative toxicity of trivalent and pentavalent inorganic and methylated arsenicals in rat and human cells. *Arch. Toxicol.*, *74*, 289-299.

- (70) Mass, M. J., Tennant, A. H., Roop, B. C., Cullen, W. R., Styblo, M., Thomas, D. J., and Kligerman, A. D. (2001) Methylated trivalent arsenic species are genotoxic. *Chem. Res. Toxicol.*, *14*, 355-361.
- (71) Petrick, J. S., Jagadish, B., Mash, E. A., and Aposhian, H. V. (2001) Monomethylarsonous acid [MMA(III)] and arsenite: LD50 in hamsters and in vitro inhibition of pyruvate dehydrogenase. *Chem. Res. Toxicol.*, *14*, 651-656.
- (72) Dopp, E., Hartmann, L. M., Florea, A. M., von Recklinghausen, U., Pieper, R., Shokouhi, B., Rettenmeier, A. W., Hirner, A. V., and Obe, G. (2004) Uptake of inorganic and organic derivatives of arsenic associated with induced cytotoxic and genotoxic effect in Chinese hamster ovary (CHO) cells. *Toxicol. Appl. Pharmacol.*, *201*, 156-165.
- (73) Dopp, E., Hartmann, L. M., Von Recklinghausen, U., Florea, A. M., Rabieh, S., Zimmerman, U., Shokouhi, B., Yadav, S., Hirner, A. V., and Rettenmeier, A. W. (2005) Forced uptake of trivalent and pentavalent methylated and inorganic arsenic and its cyto-/genotoxicity in fibroblasts and hepatoma cells. *Toxicol. Sci.*, *87*, 46-56.
- (74) Dopp, E., Von Recklinghausen, U., Diaz-Bone, R., Hirner, A. V., and Rettenmeier, A. W. (2010) Cellular uptake, subcellular distribution and toxicity of arsenic compounds in methylating and non-methylating cells. *Environ. Res.*, *110*, 435-442.
- (75) Muniz Ortiz, J. G., Wallace, K. A., Leinisch, F., Kadiiska, M. B., Mason, R. P., and Kligerman, A. D. (2013) Catalase has a key role in protecting cells from the genotoxic effects of monomethylarsonous acid: a highly active metabolite of arsenic. *Environ. Mol. Mutagen.*, *54*, 317-326.
- (76) Aposhian, H. V., Zakharyan, R. A., Avram, M. D., Kopplin, M. J., and Wollenberg, M. L. (2003) Oxidation and detoxification of trivalent arsenic species. *Toxicol. Appl. Pharmacol.*, *193*, 1-8.
- (77) Pi, J., Diwan, B. A., Sun, Y., Liu, J., Qu, W., He, Y., Styblo, M., and Waalkes, M. P. (2008) Arsenic-induced malignant transformation of human keratinocytes: involvement of Nrf2. *Free Radic. Biol. Med.*, *2008*, 651-658.
- (78) Wen, G., Calaf, G. M., Partridge, M. A., Echiburu-Chau, C., Zhao, Y., Huang, S., Chai, Y., Li, B., Hu, B., and Hai, T. K. (2008) Neoplastic transformation of human small airway epithelial cells induced by arsenic. *Mol. Med.*, *14*, 2-10.
- (79) Huang, C., Ke, Q., Costa, M., and Shi, X. (2004) Molecular mechanisms of arsenic carcinogenesis. *Mol. Cell. Biochem.*, *255*, 57-66.
- (80) Shen, S., Lee, J., Weinfeld, M., and Le, X. C. (2008) Attenuation of DNA damage-induced p53 expression by arsenic: a possible mechanism for arsenic co-carcinogenesis. *Mol. Carcinog.*, *47*, 508-518.
- (81) Li, Y., Jiang, R., Zhao, Y., Xu, Y., Ling, M., Pang, Y., Shen, L., Zhou, Y., Zhang, J., Zhou, J., Wang, X., and Liu, Q. (2012) Opposed arsenite-mediated regulation of p53-

survivin is involved in transformation, DNA damage, or apoptosis in human keratinocytes. *Toxicology*, 300, 121-131.

- (82) Wang, Z., Zhou, J., Lu, X., Gong, Z., and Le, X. C. (2004) Arsenic speciation in urine from acute promyelocytic leukemia patients undergoing arsenic trioxide treatment. *Chem. Res. Toxicol.*, 17, 95-103.
- (83) Bailey, K. A., Hester, S. D., Knapp, G. W., Owen, R. D., and Thai, S.-F. (2010) Gene expression of normal human epidermal keratinocytes modulated by trivalent arsenicals. *Mol. Carcinog.*, 49, 981-998.